

The effect of proof-testing on the Weibull distribution

D. G. HARLOW

Department of Mechanical Engineering and Mechanics, Center for the Application of Mathematics, Lehigh University, Bethlehem, Pennsylvania 18015, USA

The statistical aspects of proof-testing as they relate to the Weibull cumulative distribution function (cdf) are described. Properties of the truncated Weibull cdf which arise from proof-testing are presented. The need for accurate parameter estimation techniques is discussed, and the maximum likelihood (ML) method is developed for this application. Two examples are given which demonstrate the applicability and usefulness of the truncated Weibull cdf. One example, developed from proof-testing single filaments, illustrates the results for ungrouped data. The other, taken from an application of optical image analysis of creep cavities in stainless steel, is an example of the analysis for grouped data.

1. Introduction

Proof-testing has become one of the standard practices in many engineering applications. Some of the applications for which proof-testing is quite important include the various uses of modern composite materials [1], the many functions realized by ceramics [2, 3], and optical fibres [4, 5]. The typical reasoning for employing proof-testing is as follows. Within a population there may be specimens which are sufficiently weak that the function of the material is severely impaired. Proof-testing the population will necessarily remove these weak specimens. Furthermore, there is a guaranteed minimum strength or time to failure which ensures the successful operation of the material beyond that value. Another heuristic scenario, at least for composite materials, concerns weak flaw sites within the material. The effect of the weak flaws may be minimized by applying a controlled proof-load which is a fraction of the mean failure load. When the composite is loaded thereafter in service, the failure process is assumed to result from flaws which require strengths or times to failure in excess of the proof-load conditions.

Based upon theoretical and empirical justifications for engineering applications, the two-parameter Weibull cumulative distribution function (cdf) has become one of the more popular models in use. Consequently, it is very natural for the Weibull cdf to arise as one of the basic models in cases for which proof-testing is helpful. Therefore, assume that X is a random variable whose cdf is the two-parameter Weibull cdf given by

$$F(x) = P\{X \leq x\} = 1 - \exp[-(x/\beta)^\alpha] \quad x \geq 0, \quad (1)$$

where α and β are the shape and scale parameters, respectively.

Let x_p be the proof-load applied to a specimen sampled from a population which is characterized by Equation 1. The conditional reliability for a specimen

with random variable X is the reliability for the residual of X , given that the specimen has been subjected to x_p . Symbolically the conditional reliability is

$$R(x|x_p) = P\{X > x | X > x_p\} = \exp\{-[(x/\beta)^\alpha - (x_p/\beta)^\alpha]\} \quad x \geq x_p \quad (2)$$

and the conditional cdf is

$$F(x|x_p) = 1 - \exp\{-[(x/\beta)^\alpha - (x_p/\beta)^\alpha]\} \quad x \geq x_p \quad (3)$$

Notice that Equation 3 is a truncated cdf. Truncation occurs when it is impossible to select a sample or when it is impossible to observe a sample in some subset of the original sample space. In this case, the original sample space of $[0, \infty)$ is truncated at x_p so that the residual sample space is $[x_p, \infty)$. Herein, the truncation is assumed to occur only in the lower tail of the cdf. However, others, e.g. [6], have considered truncations in the upper tail to model random variables for which there is a maximum upper limit.

Most authors use Equation 3 or a related form for their proof-test analysis; see [1-5] as examples. However, very few authors adequately focus upon the properties of Equation 3. Nelson [7] is one exception. He presents a few of the simple properties and the conditional expected value. He does not discuss higher order moments, and he only gives trivial examples for applications of the truncated cdf. There is no discussion of estimation techniques for the parameters. The only paper which discusses estimation of the parameters in the truncated Weibull cdf is by Charernkavanich and Cohen [8]. Their work includes truncation in the upper tail and in the lower tail. They develop two estimation techniques and asymptotic sampling errors for the estimates. However, they assume that the truncation point is unknown and must be estimated from the data as well as the other parameters. This is unreasonable for proof-testing

applications because the proof-load is known, and the truncated Weibull cdf has only two parameters to estimate. Furthermore, their examples are sterile simulations motivated by their mathematical analyses rather than physically realizable ones supported by experimental data.

In practice, essentially no one engages in any discussion concerning techniques for estimating the parameters in Equation 3. A common implicit assumption is that the parameters α and β can be determined by analysis of failure data taken when no proof-load is applied and that those parameters are not effected by proof-loading. This assumption is suspect. Metals frequently undergo strain hardening or microyielding, and in some cases, these phenomena may occur at relatively low stress levels. Either of these conditions will tend to improve the reliability of the material. It is reasonable that these conditions must necessarily affect the parameters in Equation 3. For composite materials there may be considerable micromechanical damage as a result of proof-loading and, in fact, the reliability can be substantially reduced [9, 10]. Again, the proof-loading does affect the statistical parameters. Thus, properly estimating the statistical parameters of the material with and without proof-testing can yield additional information about the material performance. In any case, the parameters should be estimated from the actual data and not inferred from data obtained under other loading conditions.

Another closely related problem is incurred whenever measurements are made at or near the limits of capability of the instrument. There very well may be measurable physical quantities which are truncated simply due to limitations in the instrumentation. This truncation is analogous to the proof-loading described above; however, there is no equivalent experiment to the case of no proof-loading. The truncation problem cannot be removed or ignored.

Yet another related truncation problem occurs in experimental measurements when the desired quantity to be measured is contaminated by extraneous material. Often the contaminants and the desired quantities

are indistinguishable by the instrumentation. In such cases, the data are frequently truncated to remove any contribution to the measurements and ensuing analyses from the contaminants. Without the truncation, analysis of the data becomes considerably more difficult.

The purpose of this paper is to characterize the truncated Weibull cdf Equation 1.3 which results in proof-testing and related problems. Both numerical and analytical results for the characterization are given. The maximum likelihood estimator (MLE) for the parameters in Equation 3 is developed for both grouped and ungrouped data. Finally, two examples are considered: one is from proof-testing single filaments and one is from an instrumentation truncation problem.

2. Properties of the truncated Weibull cdf

The truncated Weibull cdf in Equation 3 obviously is identical to the standard two-parameter Weibull cdf when $x_p = 0$. To gain an appreciation for the differences between the two forms. Fig. 1 is a graph on Weibull probability paper of Equation 3 for $\alpha = 5$ and for $x_p = 0.0, 0.2\beta, 0.4\beta, 0.6\beta$ and 0.8β . Notice that the upper tail is identical for each cdf, and that the lower tail rapidly turns downward as x approaches x_p . For x slightly greater than x_p , the improvement in the reliability of the proof-tested specimens compared to that for no proof-testing is manifest. For an applied load less than x_p the truncated reliability is unity because the specimen has already been proof-loaded beyond that load. Similar observations could be made by comparing the probability density functions (pdf). The pdf of Equation 3 is

$$f(x|x_p) = (\alpha/\beta)(x/\beta)^{\alpha-1} \exp \{ -[(x/\beta)^\alpha - (x_p/\beta)^\alpha] \} \quad x \geq x_p \quad (4)$$

For the sake of completeness, the major properties of the truncated Weibull are given with little or no comment. The 100 q th percentile x_q is easily seen to be

$$x_q = \beta[(x_p/\beta)^\alpha - \ln(1 - q)]^{1/\alpha} \quad (5)$$

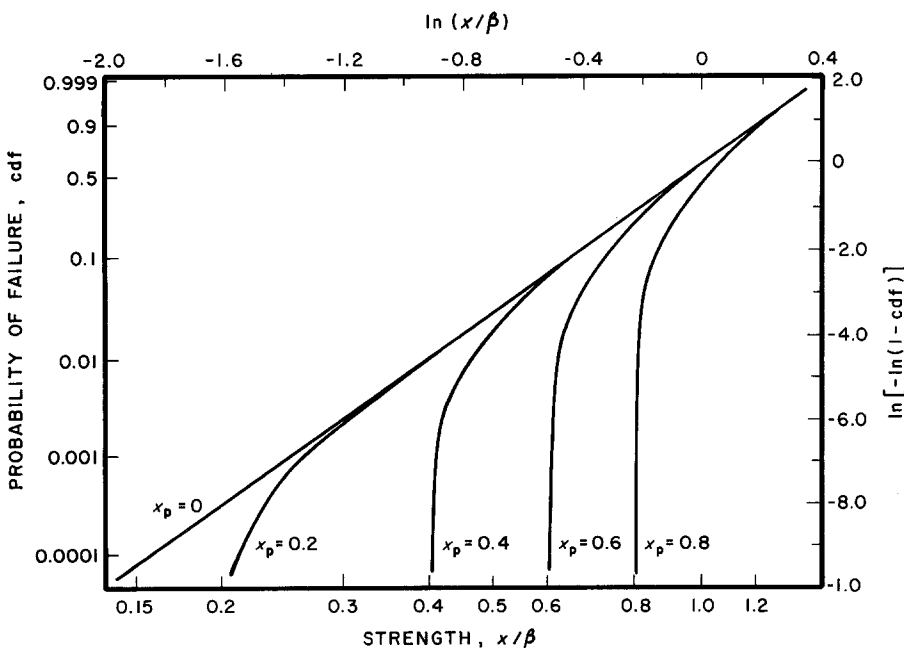


Figure 1 Comparison of the standard two-parameter Weibull cdf with the two-parameter truncated Weibull cdf. $F(x|x_p) = 1 - \exp \{ -[(x/\beta)^\alpha - (x_p/\beta)^\alpha] \}$, $\alpha = 5.0$.

The mode x_m is inferred from the pdf (Equation 4) to be

$$x_m = \beta[(\alpha - 1)/\alpha]^{1/\alpha} \quad \alpha \geq 1 \quad (6)$$

no solution exists when $\alpha < 1$. It should be noticed that the mode does not depend upon the proof-load x_p . For practical purposes, when $\alpha \geq 2$, $x_m > x_p$. The truncated hazard function $h(x|x_p)$ naturally is given by

$$h(x|x_p) = (\alpha/\beta)(x/\beta)^{\alpha-1} \quad x \geq x_p \quad (7)$$

Except for the domain of definition, Equation 7 is identical to the hazard function for the standard two-parameter Weibull cdf.

The most important quantities which characterize the cdf are the moments. Thus, using the pdf in Equation 4, the truncated moments for $k \geq 1$ are defined by the conditional expectations as follows:

$$\begin{aligned} E(X^k|x_p) &= \int_{x_p}^{\infty} x^k f(x|x_p) dx \\ &= \beta^k \Gamma(1 + k/\alpha) \exp[(x_p/\beta)^\alpha] \\ &\quad - \int_0^{x_p} x^k f(x|x_p) dx \end{aligned} \quad (8)$$

where $\Gamma(x)$ is the Gamma function. Again, note that when $x_p = 0$, the truncated moment reduces to the corresponding moment for the Weibull cdf. Two useful measures of central tendency are the coefficient of variation, cv , defined as

$$cv = (E\{[X - E(X|x_p)]^2|x_p\})^{1/2}/E(X|x_p) \quad (9)$$

and the coefficient of skewness, cs , defined as

$$cs = E\{[X - E(X|x_p)]^3\} / (E\{[X - E(X|x_p)]^2|x_p\})^{3/2} \quad (10)$$

The truncated moments must be computed numerically except for the exponential case when $\alpha = 1$. The integrals are well behaved, and any standard numerical integration scheme will produce acceptable results. Assume that $x_p = r\beta$ for some fraction r , so that the above can be computed. Typically $0 \leq r \leq 1$, and in fact, if the proof-load is too high the fraction of the surviving specimens is too low to be cost and operationally effective. Table I contains the mean/ β , the cv , and the cs , for a few selected values of r and α . The general trend is that as α increases, the cv decreases, and for fixed α , the cv decreases as x_p increases. Both of these conditions naturally reduce scatter. If $\alpha < 1.0$, the cs decreases as x_p increases; if $\alpha = 1.0$, cs is constant; and if $\alpha > 1.0$, the cs increases as x_p increases. Notice that for the larger values of α , the cdf is skewed to the left for small values of x_p , and it continuously becomes skewed to the right as x_p increases. Coleman [11] contains a similar table for the single case of $x_p = 0$.

3. Maximum likelihood estimation

3.1. Ungrouped data

Even though the truncated Weibull cdf in Equation 3 has only two parameters, there does not appear to be any simple way to obtain an estimate of α and β . Because the ML method is very general and very efficient, it is well-suited for this application. Let the caret

TABLE I The mean/ β , coefficient of variation cv , and coefficient of skewness cs , for the truncated Weibull cdf, where the proof-load is given by $x_p = r\beta$

α	r	mean/ β	cv	cs
0.5	0.0	2.0000	2.2361	6.6188
	0.2	3.0944	1.7086	5.6620
	0.4	3.6649	1.5367	5.3583
	0.6	4.1492	1.4216	5.1534
	0.8	4.5889	1.3347	4.9969
1.0	1.0	5.0000	1.2649	4.8699
	0.0	1.0000	1.0000	2.0000
	0.2	1.2000	0.8333	2.0000
	0.4	1.4000	0.7143	2.0000
	0.6	1.6000	0.6250	2.0000
1.5	0.8	1.8000	0.5556	2.0000
	1.0	2.0000	0.5000	2.0000
	0.0	0.9027	0.6790	1.0720
	0.2	0.9761	0.6041	1.1645
	0.4	1.0957	0.5114	1.2623
2.0	0.6	1.2363	0.4309	1.3452
	0.8	1.3896	0.3653	1.4148
	1.0	1.5517	0.3127	1.4735
	0.0	0.8862	0.5227	0.6311
	0.2	0.9170	0.4867	0.7264
5.0	0.4	0.9945	0.4159	0.8759
	0.6	1.1032	0.3427	1.0189
	0.8	1.2335	0.2792	1.1451
	1.0	1.3789	0.2276	1.2539
	0.0	0.9182	0.2291	-0.2541
10.0	0.2	0.9184	0.2286	-0.2443
	0.4	0.9242	0.2193	-0.1213
	0.6	0.9521	0.1873	0.1674
	0.8	1.0196	0.1365	0.5386
	1.0	1.1307	0.0866	0.9139
20.0	0.0	0.9513	0.1203	-0.6376
	0.2	0.9513	0.1203	-0.6367
	0.4	0.9514	0.1201	-0.6275
	0.6	0.9538	0.1156	-0.4672
	0.8	0.9770	0.0894	0.0555
	1.0	1.0624	0.0426	0.8136
	0.0	0.9735	0.0620	-0.8680
	0.6	0.9735	0.0619	-0.8598
	0.8	0.9760	0.0574	-0.5411
	1.0	1.0305	0.0212	0.7672

(\wedge) denote the MLEs, as is customary. Assume that the sample failure data (x_i ; $1 \leq i \leq n$) is complete. The parameter estimates are obtained by maximizing the likelihood function

$$L(\hat{x}; \alpha, \beta) = \prod f(x_i; \alpha, \beta|x_p), \quad (11)$$

where $f(x; \alpha, \beta|x_p)$ is the truncated Weibull pdf given in Equation 4 and where the product is over the index i , $1 \leq i \leq n$. After straightforward algebraic manipulation of Equation 11, $\hat{\alpha}$ is found as the solution of the nonlinear equation

$$\begin{aligned} [n^{-1} \sum x_i^\alpha - x_p^\alpha] [(n/\alpha) + \sum \ln(x_i)] \\ - \sum x_i^\alpha \ln(x_i) + nx_p^\alpha \ln(x_p) = 0 \end{aligned} \quad (12)$$

where the summations here and henceforth are for the index i ranging from 1 to n , unless it is noted otherwise. After obtaining $\hat{\alpha}$ from Equation 12, $\hat{\beta}$ is given by

$$\hat{\beta} = [n^{-1} \sum x_i^{\hat{\alpha}} - x_p^{\hat{\alpha}}]^{1/\hat{\alpha}} \quad (13)$$

It is advantageous to change the variables as follows: let $y_i = \ln(x_i)$, and let $y_p = \ln(x_p)$. Rewriting

Equation 12 yields

$$(1 + \alpha \bar{y}) \Sigma [\exp(\alpha y_i) - \exp(\alpha y_p)] - \alpha \Sigma [y_i \exp(\alpha y_i) - y_p \exp(\alpha y_p)] = 0 \quad (14)$$

where $\bar{y} = \Sigma y_i/n$ is the sample average of the transformed data. It is easy to see that both the first and second summations in the above difference are non-negative for $\alpha \geq 0$. Furthermore, the derivatives with respect to α of the first and second summations in Equation 14 are also non-negative for $\alpha \geq 0$. Because Equation 14 is trivially satisfied when $\alpha = 0$, then there can be at most one solution $\hat{\alpha}$, i.e. $\hat{\alpha}$ is unique, if it exists.

The remaining problem is the numerical solution. It is expedient to utilize another change of variables. Let $z_i = y_i - \bar{y}$ and $z_p = y_p - \bar{y}$. Multiplying Equation 14 by $\exp(-\alpha \bar{y})$ and rearranging the terms yields a function of α , say $h(\alpha)$, defined as

$$h(\alpha) = n(\alpha z_p - 1) \exp(\alpha z_p) + \Sigma (1 - \alpha z_i) \exp(\alpha z_i) = 0 \quad (15)$$

Equation 15 is equivalent to Equation 12; however, it is considerably more stable numerically. When $x_p = 0$, $h(\alpha)$ is identical to the equation used by McCool [12].

Because the non-zero solution to Equation 15 is unique, the standard Newton-Raphson method for finding the root is quite efficient. The speed of the convergence of the method depends upon the initial guess for the root. It is suggested that the initial guess for $\hat{\alpha}$ be

$$\hat{\alpha}_0 = [\text{cv}(n)]^{-1/0.94} \quad (16)$$

where $\text{cv}(n)$ is the sample coefficient of variation. The guess is based on the well-known approximation

$$\text{cv} \approx \alpha^{-0.94} \quad (17)$$

for the Weibull cdf Equation 1. Even with a convergence criterion of the difference between successive iterations being less than 10^{-10} , the convergence typically terminates in less than ten iterations when Equation 16 is the initial guess. Additional comments on the numerical aspects will be included along with the examples in the following section.

3.2. Grouped data

Many instruments make such a large number of measurements that the only reasonable way in which to assimilate the data is to use grouping techniques. Examples of such instruments are scanning electronic microscopes. For grouped data the likelihood function is

$$L(\bar{\alpha}; \alpha, \beta) = \Pi [R(a_{i-1}|x_p) - R(a_i|x_p)]^{d_i} \quad (18)$$

where $R(x|x_p)$ is given in Equation 2, $I_i = [a_{i-1}, a_i)$ is the i th interval of the range of the data, d_i is the number of observations which fall within I_i , and m is the total number of intervals. The index i is assumed to range from 1 to m , unless it is noted otherwise. For the truncated Weibull cdf, Equation 18 is considerably more tedious to maximize than the likelihood function for ungrouped data, Equation 11. The system of equations for which the solution is the MLE is

as follows

$$\Sigma d_i [(x_p/\beta)^\alpha \ln(x_p/\beta) + \{(a_i/\beta)^\alpha \ln(a_i/\beta) \exp[-(a_i/\beta)^\alpha] - (a_{i-1}/\beta)^\alpha \ln(a_{i-1}/\beta) \exp[-(a_{i-1}/\beta)^\alpha]\} / \{\exp[-(a_{i-1}/\beta)^\alpha] - \exp[-(a_i/\beta)^\alpha]\}] = 0 \quad (19)$$

and

$$\Sigma d_i [-(\alpha/\beta) (x_p/\beta)^\alpha + \{(\alpha/\beta) (a_{i-1}/\beta)^\alpha \exp[-(a_{i-1}/\beta)^\alpha] - (\alpha/\beta) (a_i/\beta)^\alpha \exp[-(a_i/\beta)^\alpha]\} / \{\exp[-(a_{i-1}/\beta)^\alpha] - \exp[-(a_i/\beta)^\alpha]\}] = 0 \quad (20)$$

Even though the equations cannot be simplified, the Newton-Raphson method again works well for this system. An initial guess which is analogous to Equation 16 for $\hat{\alpha}_0$ and the sample mean for $\hat{\beta}_0$ yields a similar convergence behaviour to that described above.

4. Examples

4.1. Ungrouped data

Because the fibres are primarily the load-bearing members in composite materials, their behaviour under proof-loading is critical to the entire structure under proof-loading. Phoenix and Wu [13] have done extensive testing of Kevlar fibres, and they have found the MLEs of the two-parameter Weibull cdf for their data with 79 sample points for the tensile strength of 5 cm long Kevlar fibres to be $\hat{\alpha} = 8.2$ and $\hat{\beta} = 3590$ MPa. These values were used to simulate data under proof-loading conditions to illustrate some of the key points in the development. Fig. 2 is a graph on Weibull paper of 75 simulated failure strengths and the MLE truncated Weibull fit to the data assuming that previously a proof-load of $x_p = 0.5\hat{\beta} = 1795$ MPa had been applied to the fibres. Even with this small sample size the smallest data are best characterized by the concave downward portion of the curve. Larger sample sizes definitely would appear to be non-linear. The MLEs for this example are $\hat{\alpha} = 7.9$ and $\hat{\beta} = 3611$ MPa. To demonstrate that the solution is unique, $h(\alpha)$ from Equation 15 is plotted for these data in Fig. 3.

4.2. Grouped data

High-temperature creep is a major reason for failure in turbine engines, steam pipes, and nuclear breeder reactors. The damage and ultimate failure is due to the nucleation, growth, and coalescence of voids (Liu *et al.* [14] and Fariborz *et al.* [15, 16]). Specimens subjected to creep have times to failure which vary by as much as 300%. This scatter is due to the stochastic behaviour of the voids. The voids are randomly scattered throughout each specimen, and they are randomly distributed in size. The total cavitated volume in the specimen can be related to its residual life or residual strength. Thus, the distribution of the void sizes is very important in reliability computations.

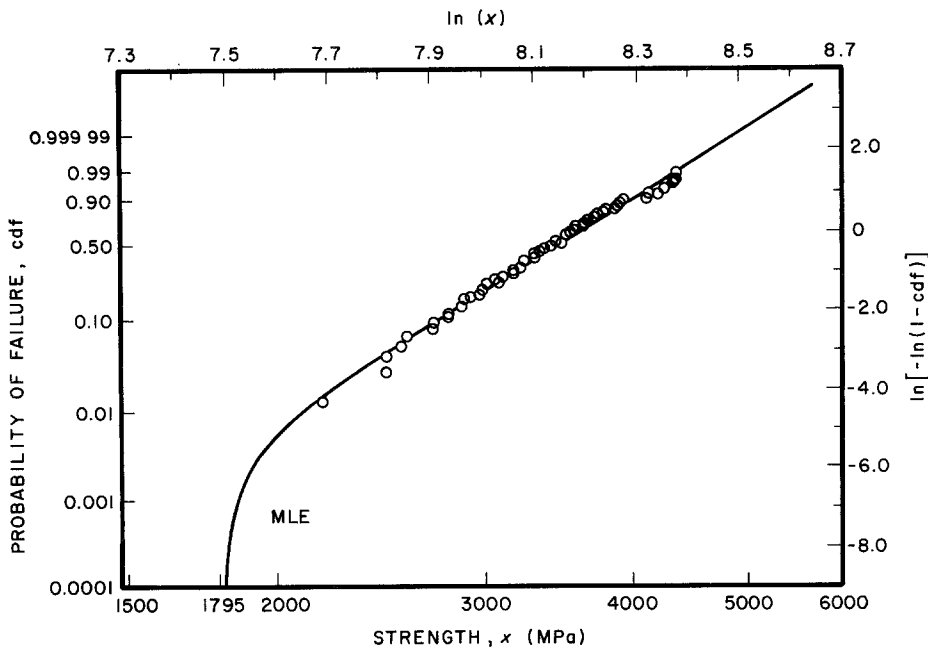


Figure 2 The MLE truncated Weibull cdf fit to simulated data for a Kevlar filament subjected to proof-loading, for 75 data. $F(x|x_p) = 1 - \exp\{-[(x/\beta)^{\hat{\alpha}} - (x_p/\beta)^{\hat{\alpha}}]\}$, $x_p = 1795$ MPa, $\hat{\alpha} = 7.9$, $\hat{\beta} = 3611$ MPa.

In attempting to model the failure mechanism, specimens are crept for some fraction of the expected failure time. The specimens are then polished and etched. Voids can be seen under a microscope; in fact, some of the larger voids can be seen with the eye. One difficulty with this method is that only the dimensions and location of the cross-section of the void in the plane of polish can be measured. That cross-section will usually not be congruent with one of the centroidal axes of the void. Hence, an estimation is required. Additionally, there will be voids which do not intersect the plane of polish. The size and number of these voids must be estimated as well. The estimation procedure is known as stereological analysis, and it yields estimates for void dimensions and the number of voids per unit volume (Liu *et al.* [17] and Cruz Orive [18, 19]).

The data to be statistically analysed are a compilation from the stereological analyses of void measurements taken from flat, plane stress tensile specimens fabricated from strip stock of a commercial heat of AISI type 304 stainless steel. The tests were conducted in air at a temperature of 600°C under constant load

creep conditions, resulting in an applied stress of 214 MPa for 776 h. For these conditions creep cavities are normally spheroidal. Consequently, the length of the major radius is of primary interest.

Unfortunately two major problems occur in the measurements which taint the void data. One problem is that the optical scanning microscope has limitations for the minimum size of a void that can be measured. Voids nucleate in time according to a non-homogeneous Poisson process which implies that ordinarily there will be voids present in the specimen which are smaller than the measurement threshold of the instrument. It is manifest that these voids are truncated from the data. The other problem is an artefact of stainless steel. Stainless steel is fairly "dirty" in that there are numerous grain-boundary inclusions and second-phase particles in the material. These are observable by the microscope. By statistically analysing several uncrept specimens, it was found that inclusions and second-phase particles with a cross-sectional area up to $10 \mu\text{m}^2$ were present in very substantial numbers. Because the goal of estimating the void distributions is to estimate residual life or

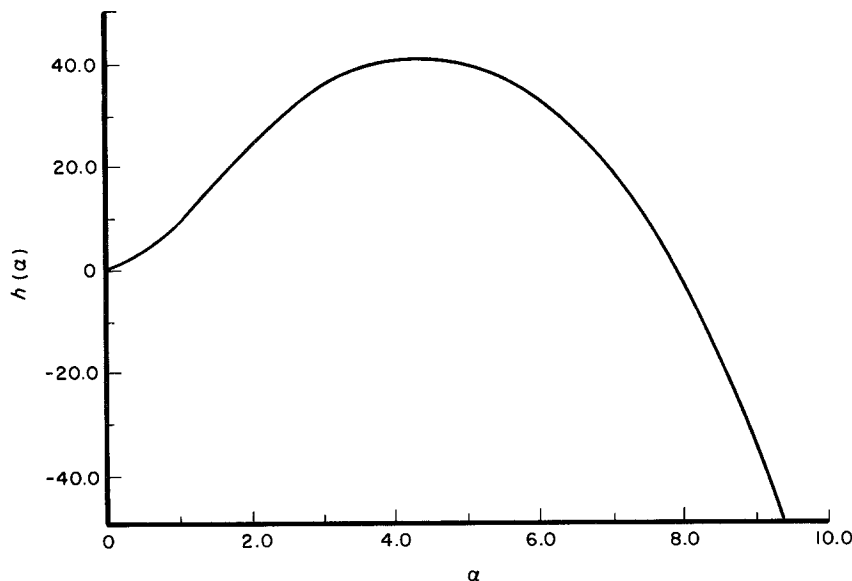


Figure 3 The non-linear function of α whose non-zero root is the MLE estimator $\hat{\alpha}$ for the Kevlar filament simulated data.

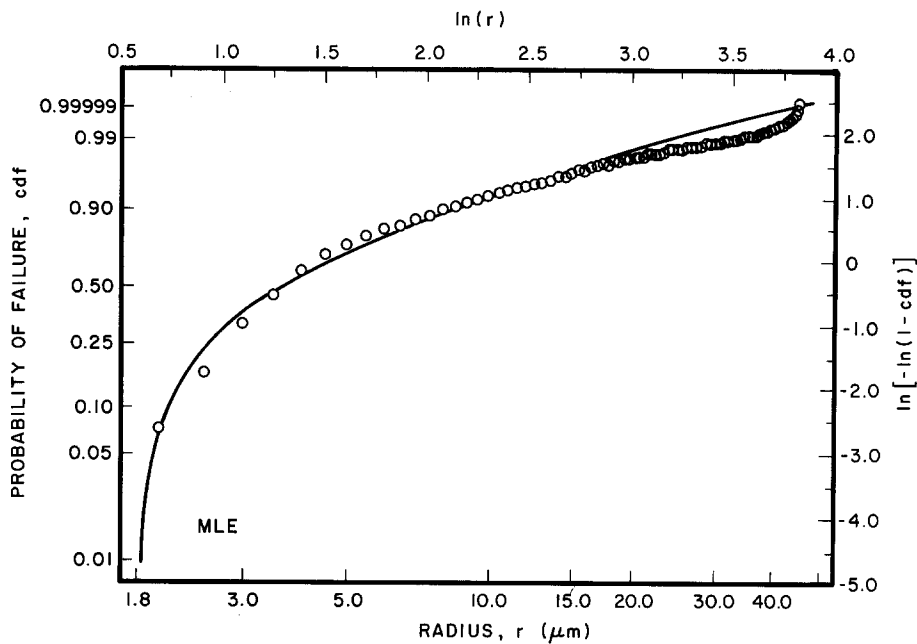


Figure 4 The MLE truncated Weibull cdf fitted to the grouped data for the cavity radii from the stereological analysis of creep cavities in AISI type 304 stainless steel. 89 groups, 108 058 data. $F(x|x_p) = 1 - \exp\{-[(x/\hat{\beta})^{\hat{\alpha}} - (x_p/\hat{\beta})^{\hat{\alpha}}]\}$, $x_p = 1.80 \mu\text{m}$, $\hat{\alpha} = 0.85$, $\hat{\beta} = 2.21 \mu\text{m}$.

residual strength and because the larger voids are primarily responsible for the amount of damage in the material, it was decided to simply truncate all the data below $10 \mu\text{m}^2$. Consequently this censoring eliminated some voids along with the "dirt". Therefore, this truncation implies that the cavity radii in the stereological analysis are truncated below $1.80 \mu\text{m}$.

Under these assumptions, the MLE method for grouped data developed herein has been employed for the cavity radius. The data and the MLE truncated Weibull cdf are presented in Fig. 4. There are a total of 108 058 cavity radii grouped into 89 class intervals. The reason for grouping is obvious. Note that the truncated Weibull fits the data quite well. The estimated parameters are $\hat{\alpha} = 0.85$ and $\hat{\beta} = 2.21 \mu\text{m}$. The estimated mean from the cdf in Equation 3 when $x_p = 1.80 \mu\text{m}$ is $4.64 \mu\text{m}$, the estimated cv is 66.4%, and the estimated cs is 2.36. The corresponding values for the standard two-parameter Weibull cdf (Equation 1) when $\hat{\alpha}$ and $\hat{\beta}$ are the same values are $2.40 \mu\text{m}$, 118.1%, and 2.56, respectively. The mean is larger by 93%, and the scatter is reduced by 44% for the truncated Weibull model. Both of these are significant. The change in cs is not as pronounced.

The large scatter indicated by the estimated cv clearly is observable from the Fig. 4. The physical reasoning for this scatter is that there are many small voids at any time due to the nucleation process. However, it is the large voids which are relatively few in number that are most critical for the reliability of the specimen. For this example, 94% of the voids have a radius less than $10 \mu\text{m}$, and the remaining voids have a radius up to $46 \mu\text{m}$. The volume of a cavity with a radius of $46 \mu\text{m}$ is approximately 20 times larger than one with a radius of $10 \mu\text{m}$. The cavity with the larger radius causes a considerably larger stress concentration in the material, and hence, it is more likely to produce further internal damage. Again, it is essential that the cavity radius cdf be estimated accurately. Thus, the method developed herein serves a critical function in the mechanical reliability estimation for the material.

5. Conclusion

A brief rationale for proof-testing has been given. Depending upon the application, the truncated Weibull cdf of Equation 3 is well-suited to represent data obtained from a truncation or proof-loading procedure. This is demonstrated by the examples in Section 4. The ML method developed herein is essential for these classes of problems. In one instance the material may undergo substantial change during proof-loading in which case the parameters estimated from the material without proof-loading cannot represent adequately the change in the proof-loaded material. In the other case it may be impossible to estimate the parameters from a population which necessarily was truncated due to instrumentation limitations or due to contamination. Although the truncated Weibull cdf is not as familiar as the standard two-parameter Weibull cdf and is not as easy to manipulate, it is to be preferred for proof-testing problems.

This paper is just an introduction to the statistics of proof-loading and its application to the Weibull cdf. There are several more aspects which need consideration. For example, confidence intervals for the estimated parameters, goodness-of-fit tests, and generalizations to other types of censoring need to be developed. This future work becomes more important as the applications of proof-testing become more critical.

Acknowledgement

This research was supported partially by the National Science Foundation under contract MSM - 8 503 411.

References

1. R. Y. KIM and W. J. PARK, *J. Compos. Mater.* **14** (1980) 69.
2. J. E. RITTER Jr, P. B. OATES, E. R. FULLER Jr and S. M. WIEDERHORN, *J. Mater. Sci.* **15** (1980) 2275.
3. E. R. FULLER Jr, S. M. WIEDERHORN, J. E. RITTER Jr and P. B. OATES, *ibid.* **15** (1980) 2282.
4. Y. MITSUNAGA, Y. KATSUYAMA, H. KOBAYASHI and Y. ISHIDA, *J. Appl. Phys.* **53** (1982) 4847.
5. Y. MIYAJIMA, *J. Lightwave Tech.* **LT-1** (1983) 340.
6. A. J. GROSS, *Technometrics* **13** (1971) 851.

7. W. NELSON, "Applied Life Data Analysis" (Wiley, New York, 1982) p. 69.
8. D. CHARERNKAVANICK and A. C. COHEN, *Commun. Statist. Theor. Meth.* **13** (1984) 843.
9. D. G. HARLOW and S. L. PHOENIX, *Int. J. Fract.* **17** (1981) 347.
10. *Idem, ibid.* **17** (1981) 601.
11. B. D. COLEMAN, *J. Mech. Phys. Solids* **7** (1958) 60.
12. J. I. McCOOL, *IEEE Trans. Reliability* **R-19** (1970) 2.
13. S. L. PHOENIX and E. M. WU, in "Proceedings of the International Union of Theoretical Applied Mechanics", edited by Z. Hashin and C. T. Herakovich (Pergamon, New York, 1983) p. 135.
14. T.-S. LIU, R. J. FIELDS, D. G. HARLOW and T. J. DELPH, *Scripta Metall.* **19** (1985) 299.
15. S. J. FARIBORZ, D. G. HARLOW and T. J. DELPH, *Acta Metall.* **33** (1985) 1.
16. *Idem, ibid.* **34** (1986) 1433.
17. T.-S. LIU, D. G. HARLOW, and T. J. DELPH, *J. Metallography* **21** (1988) 55.
18. L.-M. CRUZ ORIVE, *J. Microscopy* **107** (1976) 235.
19. *Idem, ibid.* **112** (1977) 153.

*Received 25 January
and accepted 10 June 1988*